

This article was downloaded by:

On: 25 January 2011

Access details: *Access Details: Free Access*

Publisher *Taylor & Francis*

Informa Ltd Registered in England and Wales Registered Number: 1072954 Registered office: Mortimer House, 37-41 Mortimer Street, London W1T 3JH, UK



Separation Science and Technology

Publication details, including instructions for authors and subscription information:

<http://www.informaworld.com/smpp/title~content=t713708471>

PERMEATION OF HYDROGEN THROUGH PALLADIUM/ALUMINA COMPOSITE MEMBRANES

Ting-Chia Huang^a; Ming-Chi Wei^a; Huey-Ing Chen^a

^a Department of Chemical Engineering, National Cheng Kung University, Tainan, Taiwan, R.O.C.

Online publication date: 03 December 2001

To cite this Article Huang, Ting-Chia , Wei, Ming-Chi and Chen, Huey-Ing(2001) 'PERMEATION OF HYDROGEN THROUGH PALLADIUM/ALUMINA COMPOSITE MEMBRANES', *Separation Science and Technology*, 36: 2, 199 – 222

To link to this Article: DOI: 10.1081/SS-100001075

URL: <http://dx.doi.org/10.1081/SS-100001075>

PLEASE SCROLL DOWN FOR ARTICLE

Full terms and conditions of use: <http://www.informaworld.com/terms-and-conditions-of-access.pdf>

This article may be used for research, teaching and private study purposes. Any substantial or systematic reproduction, re-distribution, re-selling, loan or sub-licensing, systematic supply or distribution in any form to anyone is expressly forbidden.

The publisher does not give any warranty express or implied or make any representation that the contents will be complete or accurate or up to date. The accuracy of any instructions, formulae and drug doses should be independently verified with primary sources. The publisher shall not be liable for any loss, actions, claims, proceedings, demand or costs or damages whatsoever or howsoever caused arising directly or indirectly in connection with or arising out of the use of this material.

PERMEATION OF HYDROGEN THROUGH PALLADIUM/ALUMINA COMPOSITE MEMBRANES

Ting-Chia Huang,* Ming-Chi Wei, and Huey-Ing Chen

Department of Chemical Engineering, National Cheng
Kung University, Tainan, Taiwan 70101, R.O.C.

ABSTRACT

In this study, the Pd/alumina composite membranes for hydrogen separation were prepared on a disk-type of α -alumina porous support and supported γ -alumina membrane by electroless-plating technique, respectively. The composite membranes with thickness of palladium layer ranging from 7–15 μm are used in the gas permeation experiment under 600–669 K and 50–220 kPa. The experimental results demonstrated that the hydrogen transport through these composite membranes is mainly controlled by solution-diffusion mechanism. It also showed that the selectivity coefficient of H_2/N_2 in the composite membranes reaches to infinite. The exponential dependency of the hydrogen partial pressure on permeation rate is in the range of 0.627 to 0.688, which is somewhat above that predicted by Sievert's law. Furthermore, the apparent activation energies of hydrogen permeation from the experimental results are within 8.8–9.3 kJ/mol. Additionally, the transport behavior of hydrogen through the bulk Pd layer of Pd/alumina composite membranes were analyzed based on the resistance model. Consequently, the hydrogen flux through a Pd/ alumina composite membrane, with

*Corresponding author. E-mail: tchuang@mail.ncku.edu.tw

a palladium film of $7 \mu\text{m}$ thick, deviated from Sievert's law. In addition, the hydrogen flux through thick Pd film ($15 \mu\text{m}$) was observed to be proportional to the difference in the square root of the hydrogen pressure on either side of the film, in accordance with Sievert's law.

Key Words: Pd/Al₂O₃ composite membranes; Palladium membrane; Hydrogen permeability

INTRODUCTION

In recent years, the use of Pd-based membranes in the separation of hydrogen and catalytic membrane reactor has received increasing attention. In order to increase the hydrogen permeation rate and retain the high permselectivity of Pd-based membranes, it is necessary to reduce the thickness of the Pd film. However, very thin membranes have the drawback of low mechanical strength. To overcome this limitation of low mechanical strength and also to enhance the permeation rate of hydrogen, Pd-based film were deposited on a mechanically resistant porous support. These membranes have high permselectivity and permeation rate and exhibit good mechanical and thermal stabilities at high temperatures. There are several techniques for the preparation of Pd-based composite membranes. Many investigators prepared Pd-based composite membranes by the electroless plating technique on microporous glass (1,2), porous stainless steel (3–5), and anodic alumina (6–11) supports. Yan and his coworker (12) deposited a Pd film on porous α -alumina support by metal-organic chemical vapor deposition method. A sputtering method was used to deposit a Pd-based film on the anodic alumina support by Konno et al. (13).

The Pd/Al₂O₃ composite membranes have a very thin, dense Pd skin layer integrated with a porous Al₂O₃ support. The permeation of hydrogen through the porous Al₂O₃ support can be described by phenomenological equation in which the hydrogen flux is proportional to the driving force, that is, the pressure difference across the Al₂O₃ support. The dust-gas model (14,15) has been used to analyze gases transport through a porous media in terms of Knudsen flow and viscous flow (16). Additionally, the permeation of hydrogen through dense membranes is analyzed using the solution-diffusion mechanism first proposed by Thomas Graham in 1888. In this case, the permeation rate of hydrogen through dense Pd-based film is proportional to the square root of pressure difference, that is, the relationship between hydrogen flux and driving force can be described by the Sievert's law (17,18). Also, a few experimental studies (2,5,9,11–13,19–21) have been reported in the literature on hydrogen transport through Pd-based composite



membranes. It was found that the exponential dependency of the partial pressure of hydrogen on hydrogen flux, n , was ranging from 0.5 to 1.0.

In this study, the Pd/Al₂O₃ composite membranes with different thickness of Pd layer on α -Al₂O₃ support and supported γ -Al₂O₃ membrane were prepared by electroless plating. Various composite membranes with different thicknesses of Pd layer and support were used for the permeation study. The hydrogen permeation behaviors through these composite membranes were investigated to understand the influence of the mass transfer resistance of α -Al₂O₃ support. Furthermore, the permeation mechanism of hydrogen through Pd/Al₂O₃ composite membranes was also discussed.

THEORETICAL CONSIDERATION

The Pd/Al₂O₃ composite membranes consisted of the dense part of the Pd membrane and the porous part of the Al₂O₃ support. Therefore, two parts of transport mechanism are taken into account for the permeation of gas.

Gas permeation in a porous medium:

The permeation of gases through a porous medium can be described by Poiseuille flow and Knudsen diffusion. The relative contribution of Knudsen diffusion to the Poiseuille flow on the overall transport rate depends on the Knudsen number, Kn , which is defined as the ratio of mean free path of the gas molecules, λ , to the pore radius of the medium, r , that is

$$Kn = \frac{\lambda}{r} \quad (1)$$

where

$$\lambda = \left(\frac{16\mu}{5\pi P_{AVE}} \right) \left(\frac{\pi RT}{2M} \right) \quad (2)$$

P_{AVE} is the average pressure across the medium, μ is the gas viscosity, T is the absolute temperature, M is the gas molecular mass, and R is the universal gas constant.

If the Knudsen number is much larger than unity, that is, $Kn \gg 1$, the gas molecules collide with the pore wall much more frequently than with each other. This transport mechanism of gas is the Knudsen flow. If the Knudsen number is much smaller than unity, that is, $Kn \ll 1$, the Poiseuille flow is the dominant mechanism. However, the transition region between Knudsen and Poiseuille occurs mainly in the range of $0.01 < Kn < 10$.

Several models have been used to describe the transition region. The conventional starting point for the description of gas permeation through porous media



is the dust gas model (14,15). In this case, the rate of gas permeation per unit area or gas flux, J , is expressed in terms of Darcy's law as follows:

$$J = F_P(P_h - P_l) \quad (3)$$

where F_P is the permeability and P_h and P_l are the partial pressures of gas in the sides of high pressure and low pressure, respectively.

In our previous work (16), the permeation of hydrogen and nitrogen through the porous α -Al₂O₃ support and supported γ -Al₂O₃ membrane under room temperature and various pressures had been investigated. It showed that the permeation of gases through these media was mainly described by Poiseuille flow and Knudsen flow. The permeability can be expressed as the sum of the Poiseuille flow, F_{PV} , P_{AVE} , and Knudsen flow, F_{PK} :

$$F_P = F_{PK} + F_{PV}P_{AVE} \quad (4)$$

in which

$$F_{PK} = \left(\frac{2\epsilon r}{3\tau LRT} \right) \left(\frac{8RT}{\pi M} \right)^{0.5} \quad (5)$$

and

$$F_{PV} = \frac{\epsilon r^2}{8\tau \mu LRT} \quad (6)$$

where ϵ is the medium porosity, τ the tortuosity factor of pores (for cylindrical perpendicular pores, the tortuosity is equal to unity), and L the media thickness.

Rearranging Equations (5) and (6), the mean pore radius of the membrane can be written in terms of F_{PV} and F_{PK} as:

$$\frac{F_{PV}}{F_{PK}} = \frac{3}{16} \left(\frac{\pi M}{8RT} \right)^{0.5} \left(\frac{r}{\mu} \right) \quad (7)$$

Then using the mean pore radius, the tortuosity factor of pores can be calculated from the following equation

$$\epsilon = 8\tau \mu LRT F_{PV} \frac{1}{r^2} \quad (8)$$

According to Equations (5) and (6), the Knudsen permeability is directly proportional to $1/(MT)^{0.5}$ and independent of mean pressure, whereas for Poiseuille flow, the permeability should be proportional to the mean pressure and $1/(\mu T)$. The selectivity coefficient (α_{ij}^*), or ideal separation factor, is defined as the ratio of permeabilities of two pure gases as follows:

$$\alpha_{ij}^* = \frac{F_{P,i}}{F_{P,j}} \quad (9)$$



If the gas flow through the porous media is merely due to Knudsen diffusion, the selectivity coefficient of two pure gases i and j can be represented by the square root of the ratio of their molecular masses, that is

$$\alpha_{ij}^* = \sqrt{\frac{M_j}{M_i}} \quad (10)$$

Hydrogen permeation in the palladium layer:

The permeation of hydrogen through the dense Pd layer usually involves several steps in series (17): 1) dissociated adsorption of molecular hydrogen on the membrane surface, 2) reversible dissolution of surface atomic hydrogen in bulk layer of palladium, 3) diffusion of atomic hydrogen in the bulk palladium layer, and 4) associated desorption of atomic hydrogen on the other surface of palladium layer. Consequently, the hydrogen flux in the Pd layer via solution-diffusion mechanism can be expressed in terms of Fick's first law as follows (18):

$$J = F_{Pl}(P_h^n - P_l^n) \quad (11)$$

where F_{Pl} is premultiplication factor and n is a constant.

Proposed mechanism of hydrogen permeation generally assumes a rate-limiting step, which may be either a surface process ($n = 1$) involving step (1), step (2) and step (4), or a bulk-diffusion process ($n = 0.5$, Sievert's law) involving step (3).

When the value of n does not depend on the temperature, the temperature dependence of the gas permeability can be expressed by an Arrhenius equation as

$$F_{Pl} = A_0 e^{\frac{-Ea}{RT}} \quad (12)$$

where A_0 is the preexponential factor and Ea is the apparent activation energy.

Summarizing the description mentioned above, the flux of hydrogen permeating through the Pd/Al₂O₃ composite membrane also could be expressed as Equation (11). In this case, the n values will be ranged between 0.5 and 1.0. To further elucidate the influence of the support transport resistance to the overall transport resistance of the composite membrane for gas permeation, a resistance model (22) is used to analyze the permeation behavior of gas through composite membrane. According to this model, the permeation behavior of gas through the composite membranes is analogous to the flow of electricity through a series-parallel array of resistors. A schematic diagram for hydrogen permeation through the palladium/α-alumina composite membrane is shown in Figure 1, where the flux corresponds to current and the pressure drop corresponds to voltage drop. Two transport resistances represented in Figure 1 are the transport resistance of hydrogen flowing through the α-alumina support, R_s , and the transport resistance of hydrogen, R_{Pd} . At steady state, the overall transport resistance, $R_{overall}$, equals



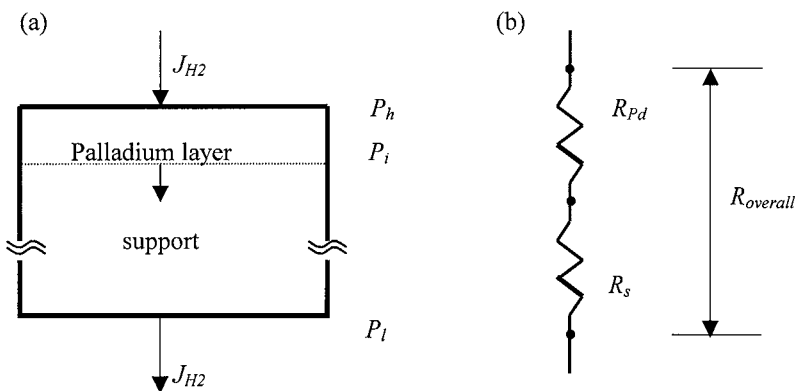


Figure 1. Schematic representation of a Pd/alumina composite membrane. a) Cross-sectional view of the Pd/alumina composite membrane, and b) electrical circuit.

to the sum of the Pd layer and porous α -alumina support. Consequently, subtracting the permeation of hydrogen through the support from overall hydrogen flux, the hydrogen flux through the bulk Pd layer of composite membrane can be obtained (23).

EXPERIMENT

Preparation of Pd/ Al_2O_3 Composite Membranes

Electroless plating technique was employed to deposit palladium film on the porous alumina support. The support was pretreated through several steps and a surface activation step prior to the electroless plating. Support was first cleaned with hydrochloric acid solution and sodium hydroxide solution, respectively, and rinsed with deionized water. An activation procedure was then adopted to seed the alumina surface with finely divided palladium nuclei, which the plating process initiated. The activation procedure consisted of the two-step immersion sequence in acidic SnCl_2 solution (96 mM) followed by acidic PdCl_2 solution (1.4 mM). After surface activation, the support was immediately rinsed with a large volume of deionized water and then dried at 100°C.

The composition of the plating solution is listed in Table 1. The plating bath was kept at $70 \pm 2^\circ\text{C}$ and was refreshed every 1 h to keep a constant depositing rate. Finally, the membranes were washed with deionized water and dried at 100°C.

Membrane Characterization

The surface morphology of membranes was observed with a scanning electron microscope (SEM) (JEOL JXA-840). In addition, the thickness of the



Table 1. Composition of the Pd Electroless Plating Baths

Component	Concentration
PdCl ₂	5.4 (g/L)
NH ₄ OH (28%)	390 (mL/L)
Na ₂ EDTA	70 (g/L)
N ₂ H ₄ (1M)	10 (mL/L)
Thiourea	0.0006 (g/L)
Loading	200 (cm ² /L)

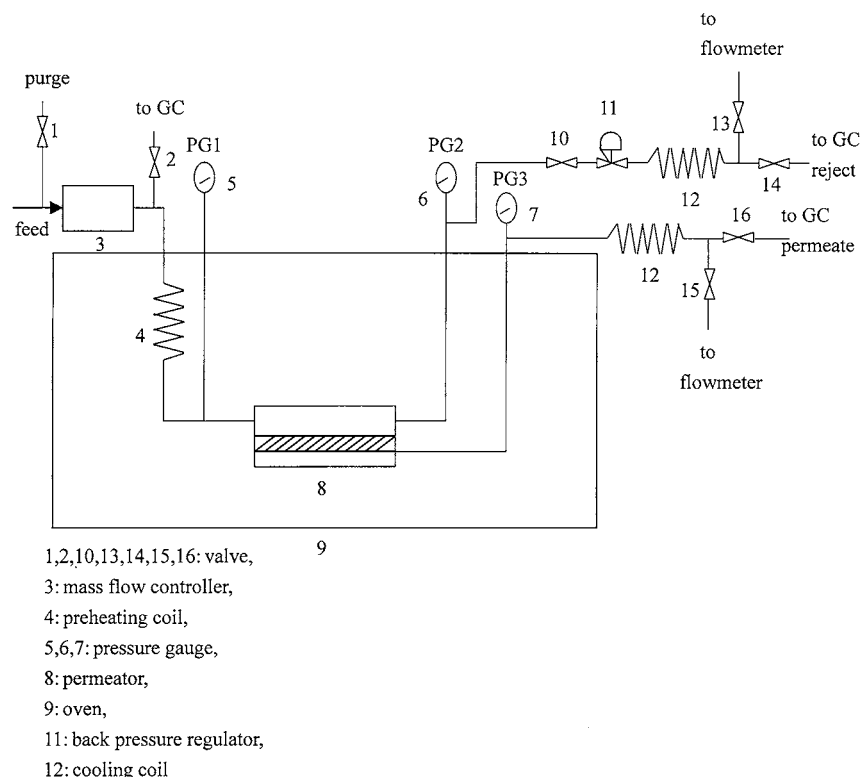


Figure 2. A schematic diagram of the experimental apparatus for gas permeability measurement.



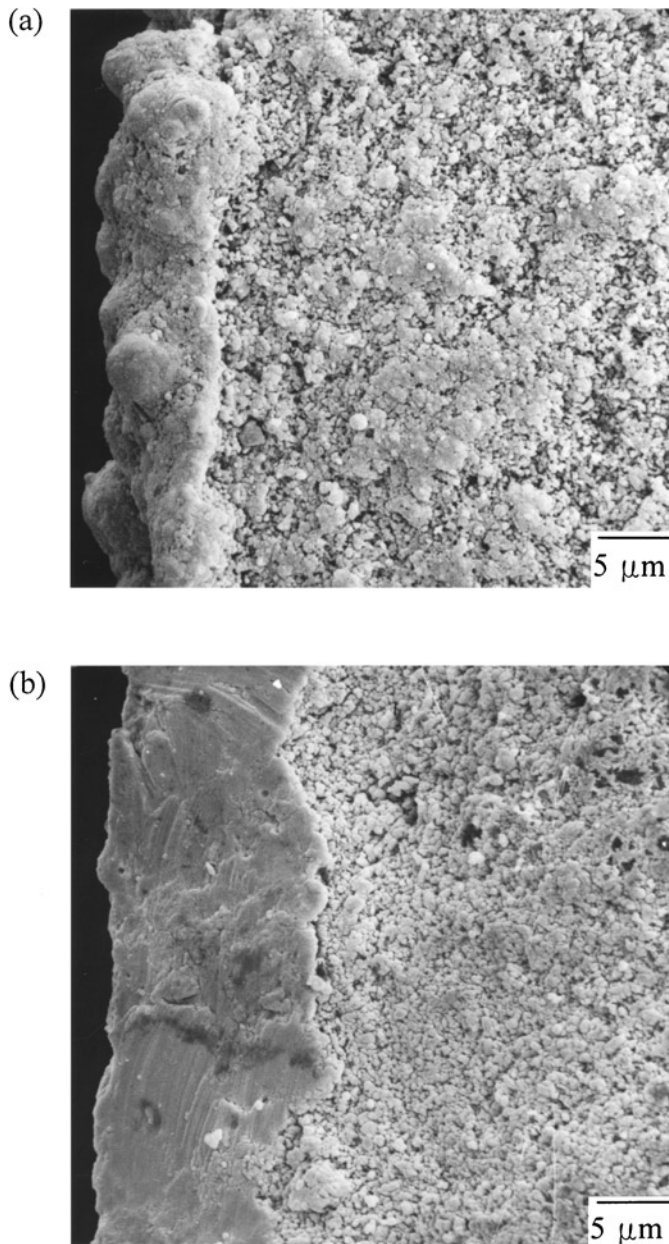


Figure 3. Scanning electron micrographs for the cross-sectional view of α -1 and α -2 membranes, respectively, a) α -1 membrane, b) α -2 membrane (magnification: 2000).



Table 2. Specification of Pd/Al₂O₃ Composite Membranes

Membrane No.	Support	Thickness of Support (mm)	<i>r</i> (nm)	ε	Plating-Time	Thickness of Pd Layer (μm)
α -1	α -Al ₂ O ₃ disk	2	95.9 ^a	0.38 ^a	1 h	7
α -2	α -Al ₂ O ₃ disk	2	95.9 ^a	0.38 ^a	2 h	15
γ -2	Supported γ -Al ₂ O ₃ membrane	2	8.6 ^b	0.15 ^b	2 h	15

^apermeation gas: H₂, N₂; permeation temperature: 523 K.

^b(25): permeation gas: He, N₂, CO₂; permeation temperature: 372 K.

palladium film was measured with EPMA from the cross-sectional view of the composite membrane. To verify the crystalline structure of the membrane prepared, X-ray diffraction (XRD) with a copper target and a nickel filter (Rigaku RX-III) was used.

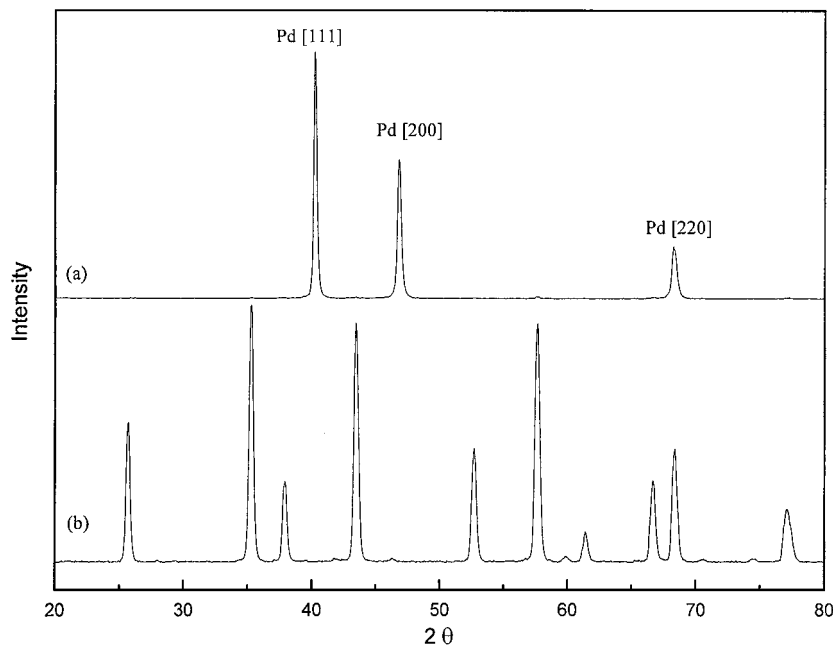


Figure 4. XRD patterns of a) the palladium/alumina composite membrane deposited for 1 h at 70°C by electroless plating technique, and b) the α -Al₂O₃ support.



Permeability Measurement

Three pieces of palladium/alumina composite membranes were used in the permeability study. The permeabilities of hydrogen and nitrogen through the membranes were measured under temperature ranges of 523–669 K and pressure differences up to 220 kPa.

A stainless-steel permeation cell with a flat membrane clamped between two pieces of gaskets was placed in a thermostat chamber. The schematic diagram of gas permeation apparatus was shown in Figure 2. The assembly of permeability testing consisted of gas cylinders, a stainless-steel permeation cell, a gas chromatograph, and a thermostat chamber. The effective area of the membrane for permeation was 4.91 cm². The upstream pressure was controlled by the regulator of gas cylinder, whereas the downstream of gas vented to air. Prior to the hydrogen permeation measurement, the flow system was preheated to the setting temperature in nitrogen

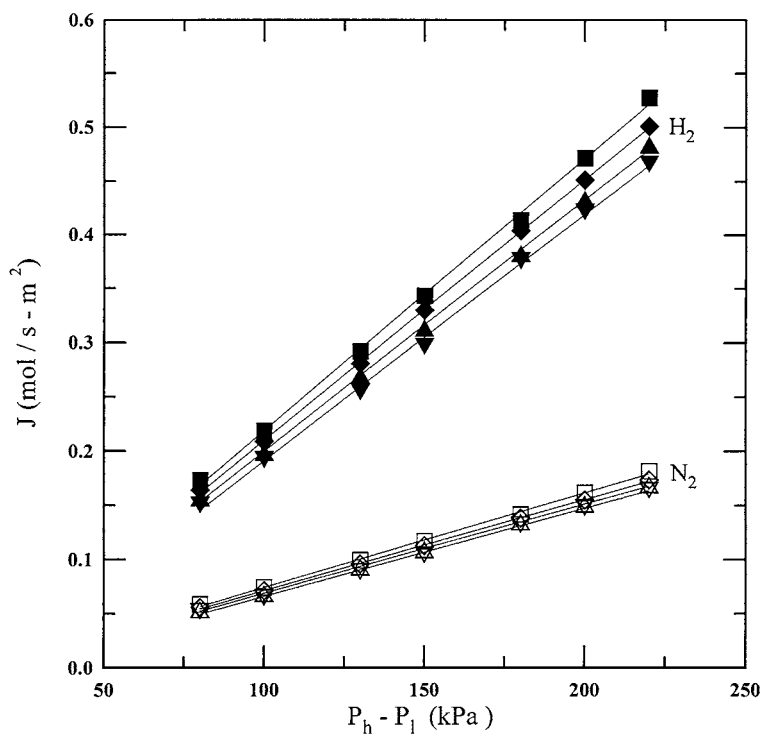


Figure 5. The hydrogen and nitrogen fluxes through α -Al₂O₃ support as a function of pressure difference at different permeation temperatures. (▽) N₂, 669 K, (△) N₂, 625 K, (◇) N₂, 573 K, (□) N₂, 523 K, (▼) H₂, 669 K, (▲) H₂, 625 K, (◆) H₂, 573 K, (■) H₂, 523 K.



atmosphere. The permeation rate of gases was measured at atmospheric pressure and ambient temperature by a soap-bubble flowmeter.

RESULTS AND DISCUSSION

Characterization of Pd/Al₂O₃ Composite Membranes

The cross-sectional views of Pd/α-Al₂O₃ composite membranes obtained by electroless-plating technique at 70°C for 1 h and 2 h, are shown in Figure 3(a) and (b), respectively. It was observed that the thickness of the Pd film on the α-Al₂O₃ support for plating 1 h (α-1) and 2 h (α-2) were 7 μm and 15 μm, respectively. Besides, for plating 2 h (γ-2), the thickness of Pd layer deposited on supported γ-Al₂O₃ membrane was determined to be about 15 μm. The thickness

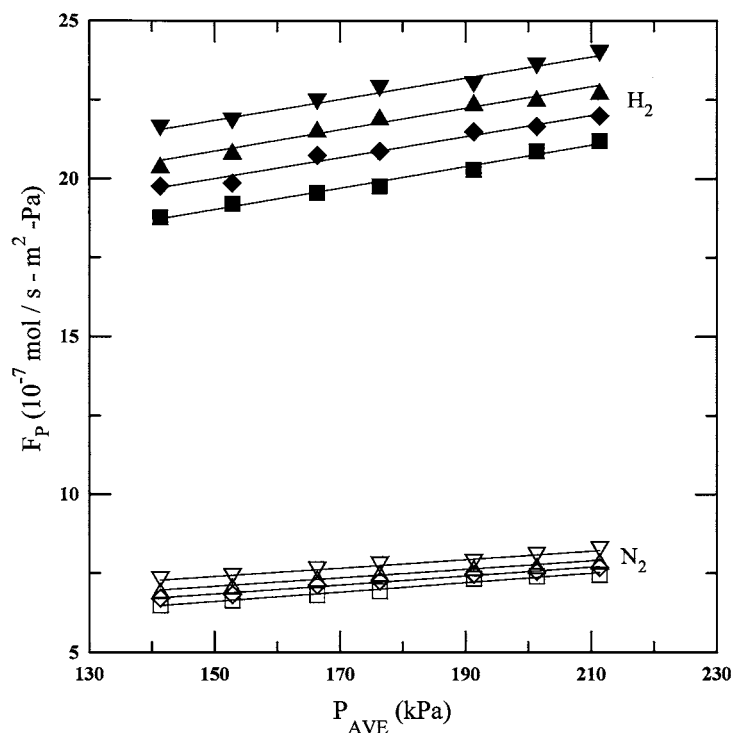


Figure 6. Gas permeabilities of H₂ and N₂ through α-Al₂O₃ support as a function of the mean pressure at different permeation temperatures. (▽) N₂, 523 K, (△) N₂, 573 K, (◇) N₂, 625 K, (□) N₂, 669 K, (▼) H₂, 523 K, (▲) H₂, 573 K, (◆) H₂, 625 K, (■) H₂, 669 K.



of Pd layers for each composite membrane, that is, α -1, α -2, and γ -2, are listed in Table 2. The results of X-ray diffraction analysis of membrane α -1 and α -Al₂O₃ support are illustrated as Figure 4 (a) and (b), respectively. Comparing Figure 4(a) and (b), it shows that there were only characteristic peaks of Pd occurring at $2\theta = 40.04, 46.54$, and 67.86 , and without any peaks of α -Al₂O₃. It strongly evidenced an f.c.c. structure of the Pd deposit. The crystallite dimension of palladium was estimated to be 36.8 nm from the width of characteristic peaks, which was very close to that obtained for pure Pd by other investigators (5,24).

Effect of Pressure and Temperature on Membrane Performance

Gas permeation through the α -Al₂O₃ support:

Figure 5 shows the dependences of hydrogen and nitrogen fluxes on transmembrane pressure difference for the α -Al₂O₃ support. It showed that the hydrogen and nitrogen fluxes through the α -Al₂O₃ support varied linearly with increasing

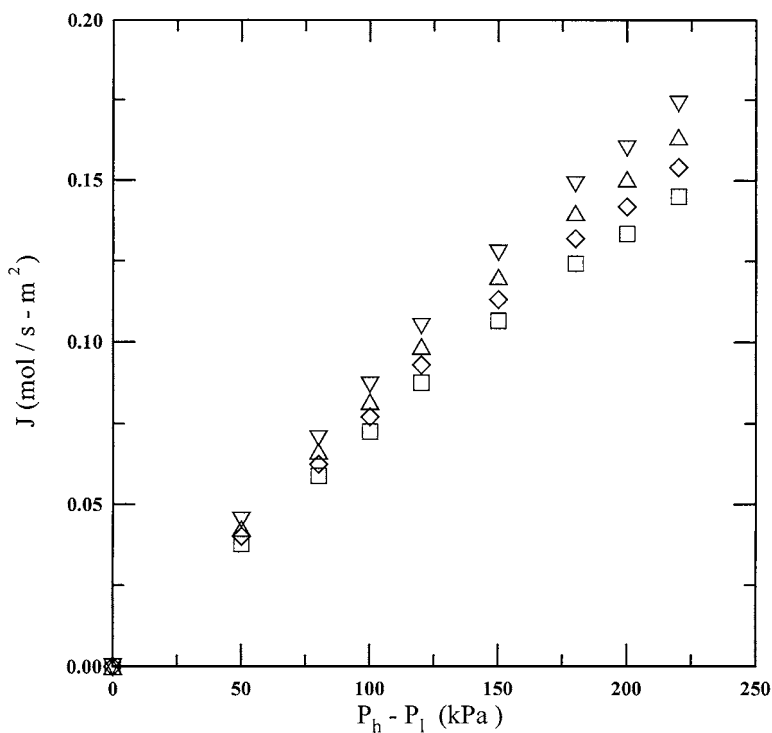


Figure 7. The hydrogen fluxes through α -1 membrane as a function of pressure difference at different permeation temperatures. (∇) 669 K, (Δ) 647 K, (\diamond) 625 K, (\square) 600 K.



pressure difference. As also can be seen from Figure 5, the hydrogen and nitrogen fluxes through the α -Al₂O₃ support were decreased with temperature; these tendencies were in accordance with Knudsen flow and Poiseuille flow behavior.

The permeabilities of hydrogen and nitrogen through the α -Al₂O₃ support at different temperatures are showed in Figure 6. The results denoted that the permeabilities varied linearly with the mean pressure. Therefore, it evidenced that the gases permeated through the α -Al₂O₃ support can be described by the combined model of Knudsen and Poiseuille mechanisms, as expressed in Equation (4). From the linear plot of F_P vs. P_{AVE} , the values of F_{PV} and F_{PK} were determined. Consequently, the mean pore radius and the porosity of supports were also determined by Equations (8) and (9) and were listed in Table 2.

Hydrogen permeation through the Pd/Al₂O₃ composite membranes:

The hydrogen fluxes at various temperatures through α -1, α -2, and γ -2 membranes were shown in Figures 7, 8, and 9, respectively. The results indicated

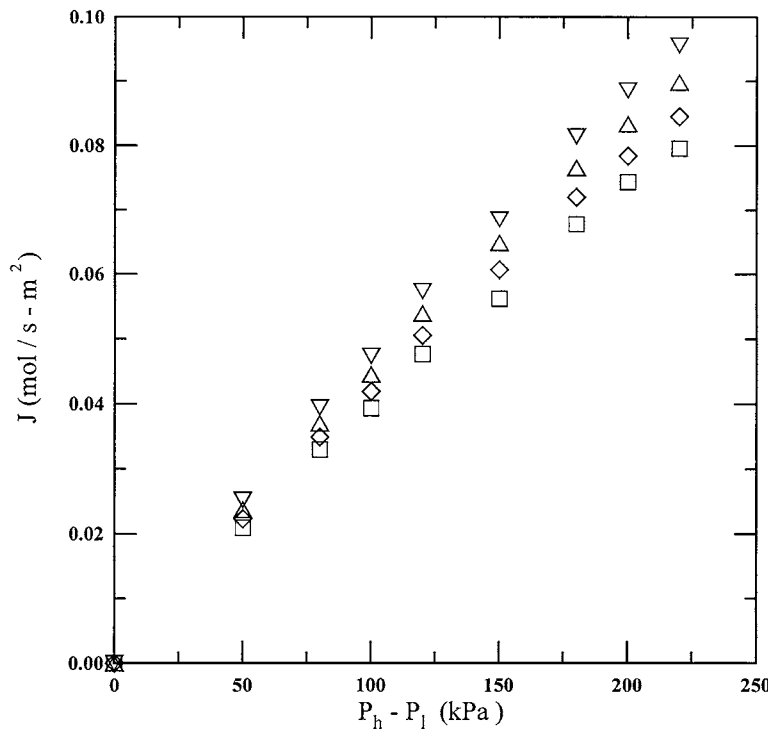


Figure 8. The hydrogen fluxes through α -2 membrane as a function of pressure difference at different permeation temperatures. (∇) 669 K, (Δ) 647 K, (\diamond) 625 K, (\square) 600 K.



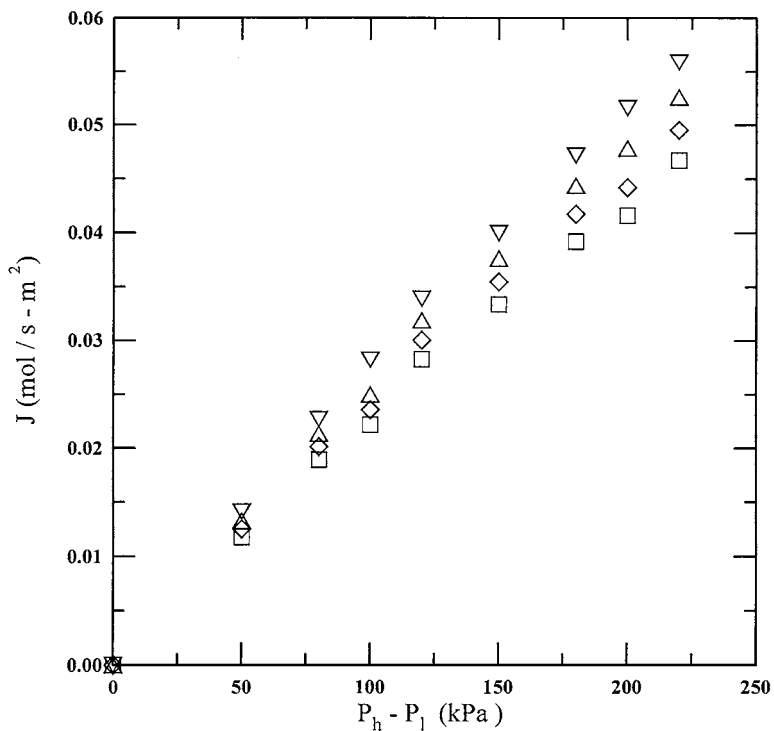


Figure 9. The hydrogen fluxes through γ -2 membrane as a function of pressure difference at different permeation temperatures. (∇) 669 K, (Δ) 647 K, (\diamond) 625 K, (\square) 600 K.

that the hydrogen fluxes through three Pd/Al₂O₃ composite membranes deviated from a straight line with increasing pressure difference. Furthermore, the hydrogen fluxes through these composite membranes were increased with increasing temperature. It was shown that the Knudsen diffusion and Poiseuille flow are no longer the dominant permeation mechanisms in the Pd/Al₂O₃ composite membranes. In

Table 3. An Example of Interface Pressure in Pd/Al₂O₃ Composite Membranes

Membrane	Temperature (K)	P_h (kPa)	P_l (kPa)	P_i (kPa)
α -1	669	201	101	149
α -2	669	201	101	128



the presence of dense Pd layer on the $\alpha\text{-Al}_2\text{O}_3$ support, the hydrogen permeation behavior in the composite membrane revealed the tendency of solution-diffusion mechanism, as expected from the Equation (11).

The hydrogen fluxes through the $\alpha\text{-Al}_2\text{O}_3$ support and three Pd composite membranes were shown in Figures 5, 7, 8, and 9, respectively. It indicated that the hydrogen fluxes through these composite membranes in each case were reduced as a result of Pd film deposition. It can be seen that for $\alpha\text{-1}$, $\alpha\text{-2}$, and $\gamma\text{-2}$ membranes, the hydrogen fluxes decreased by 64%, 80%, and 88%, respectively. The results also showed the mass transfer resistance of support could not be neglected for these composite membranes.

As illustrated in Figures 7 and 8, it finds that the measured low hydrogen flux through $\alpha\text{-2}$ membrane was evidently due to its thicker Pd layer. Comparing $\alpha\text{-2}$ with $\gamma\text{-2}$ membrane, the hydrogen fluxes in these composite membranes were

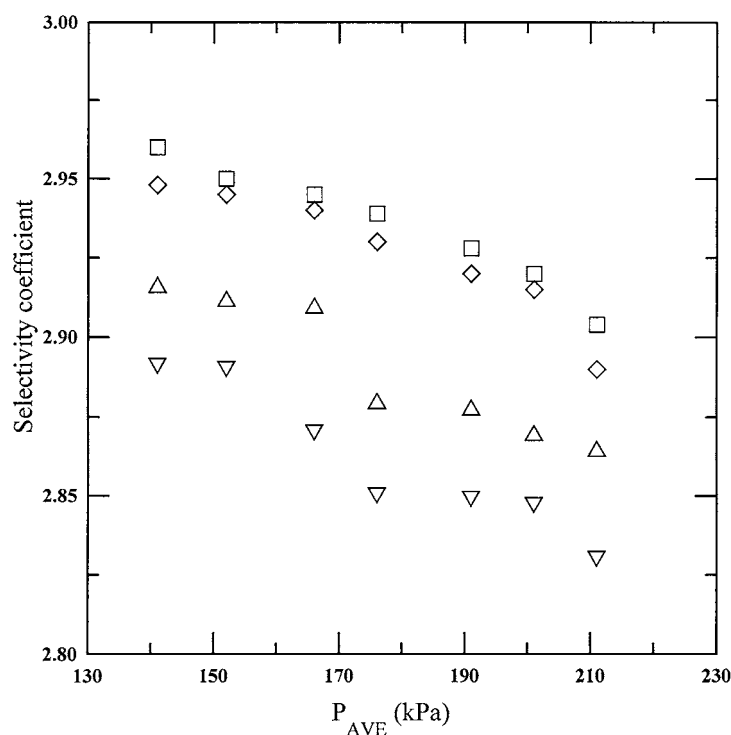


Figure 10. The selectivity coefficients of hydrogen to nitrogen as a function of mean pressure across the membrane for the $\alpha\text{-Al}_2\text{O}_3$ support at different permeation temperatures. (∇) 669 K, (\triangle) 625 K, (\diamond) 573 K, (\square) 523 K.



Table 4. Permeation Parameters for Various Palladium/Alumina Composite Membranes

Membrane Description	Temperature (K)	$F_{Pl} \times 10^5$ (mol/m ² ·s·Pa ⁿ)	n	n_{grand}
α -1	669	7.705	0.659	0.655
	647	7.613	0.656	
	625	6.850	0.659	
	600	6.591	0.657	
α -2	669	3.442	0.674	0.627
	647	3.514	0.668	
	625	3.105	0.673	
	600	2.314	0.690	
γ -2	669	2.014	0.674	0.688
	625	1.528	0.685	
	600	1.345	0.690	

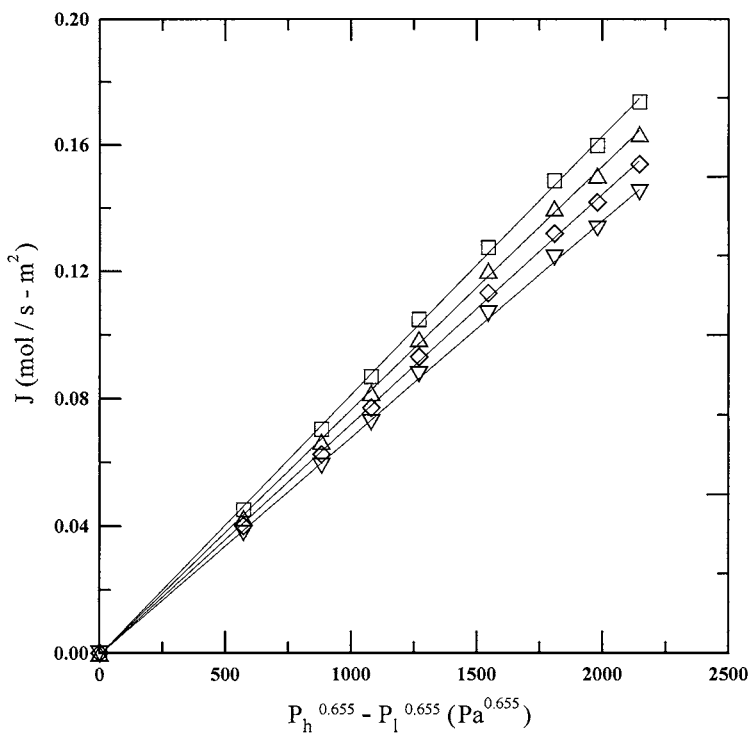


Figure 11. The dependence of hydrogen fluxes on $P_h^n - P_l^n$ at various temperatures through α -1 membrane. (□) 669 K, (△) 647 K, (◇) 625 K, (▽) 600 K.



affected by the resistance of the support. With the small pore size and porosity, the hydrogen fluxes in γ -2 membrane were smaller than that in the α -2 membrane.

From the experimental results, it can be concluded that hydrogen permeating through these Pd composite membranes was dominated by solution-diffusion mechanism, instead of a combined mechanism of Knudsen diffusion and Poiseuille flow as seen in the α -Al₂O₃ support.

Knowing J and P_i , the interface pressures, P_i , under various upstream pressures and temperatures can be evaluated (23). In Table 3 an example of interface pressure of Pd/ α -Al₂O₃ composite membrane system is shown for the case that the pressure on the upstream side was 201 kPa and the pressure on the permeate side was 101 kPa. As can be seen, the interface pressures of two membranes were much higher than the downstream pressure. It indicated, the transport resistance of support can not be neglected.

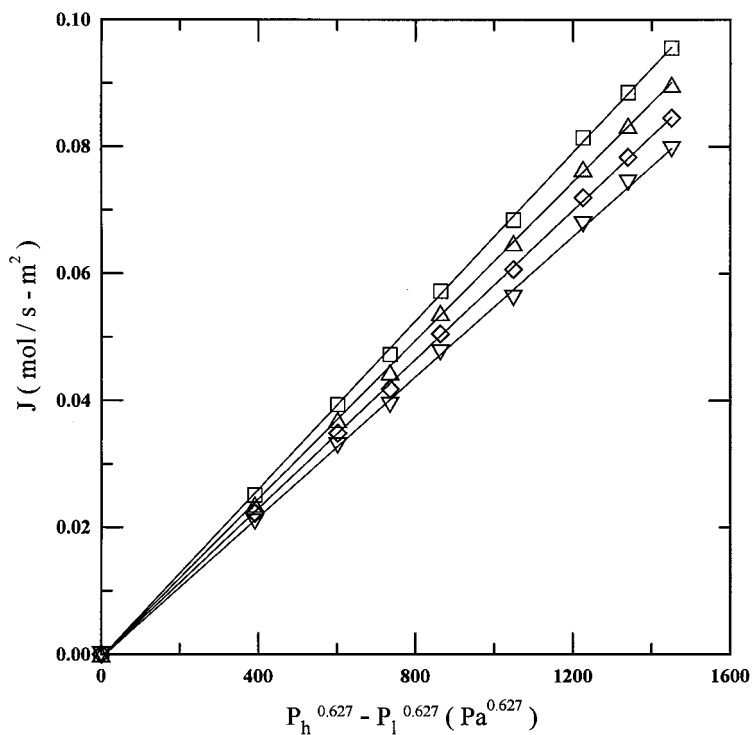


Figure 12. The dependence of hydrogen fluxes on $P_h^n - P_l^n$ at various temperatures through α -2 membrane. (□) 669 K, (△) 647 K, (◇) 625 K, (▽) 600 K.



Selectivity Coefficient of Hydrogen to Nitrogen

For $\alpha\text{-Al}_2\text{O}_3$ support:

The selectivity coefficients of hydrogen to nitrogen for the $\alpha\text{-Al}_2\text{O}_3$ support are shown in Figure 10. It can be seen that the selectivity coefficient was reduced with increasing the mean pressure, mainly due to the flow of Poiseuille model. Furthermore, the selectivity coefficients were also decreased with an increase of temperature. This behavior is consistent with Poiseuille and Knudsen model of permeation through the porous medium. Consequently, the values of selectivity coefficient of H_2/N_2 were below the theoretical value of 3.74 expected from Knudsen model.

For Pd/ Al_2O_3 composite membranes:

Three Pd composite membranes were impervious to nitrogen but permselective toward hydrogen. There was no nitrogen permeated through the Pd composite

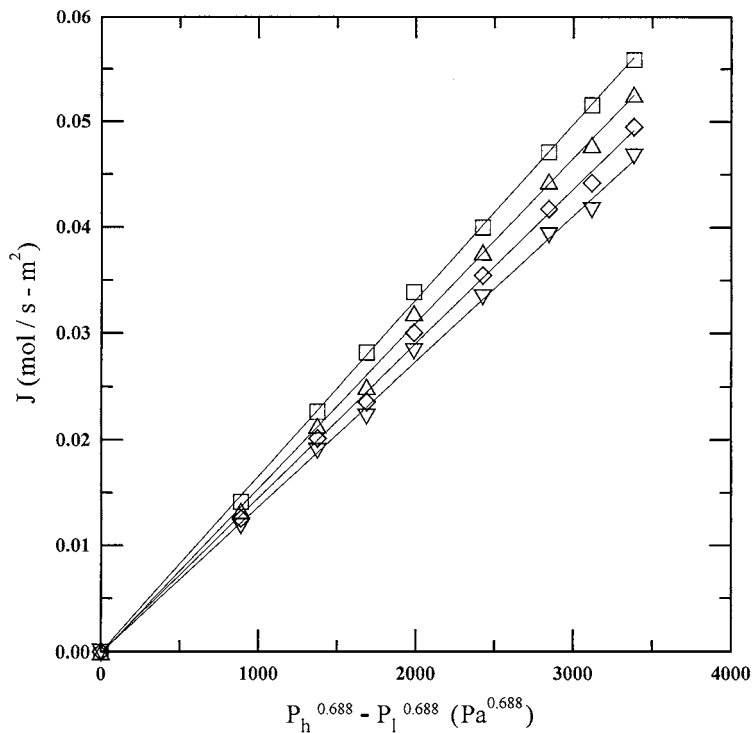


Figure 13. The dependence of hydrogen fluxes on $P_h^n - P_l^n$ at various temperatures through γ -2 membrane. (□) 669 K, (△) 647 K, (◇) 625 K, (▽) 600 K.



membrane for the pressure difference up to 220 kPa. Consequently, the selectivity coefficients of hydrogen to nitrogen through three Pd composite membranes are infinite. It also indicates that these Pd layers obtained by electroless-plating method were defect free.

Calculation of F_{Pl} and n

For Pd/Al₂O₃ composite membranes:

The hydrogen permeabilities, F_{Pl} , and n values for three Pd composite membranes were determined by nonlinear regression analysis with Equation (11) and were listed in Table 4. As can be seen, the values of n for the same composite membrane were not varied with temperature significantly. Based on this observation, the values of grand n , n_{grand} , for the α -1, α -2, and γ -2 membranes were determined as 0.655, 0.627, and 0.688, respectively. The results are shown in Figures 11, 12, and

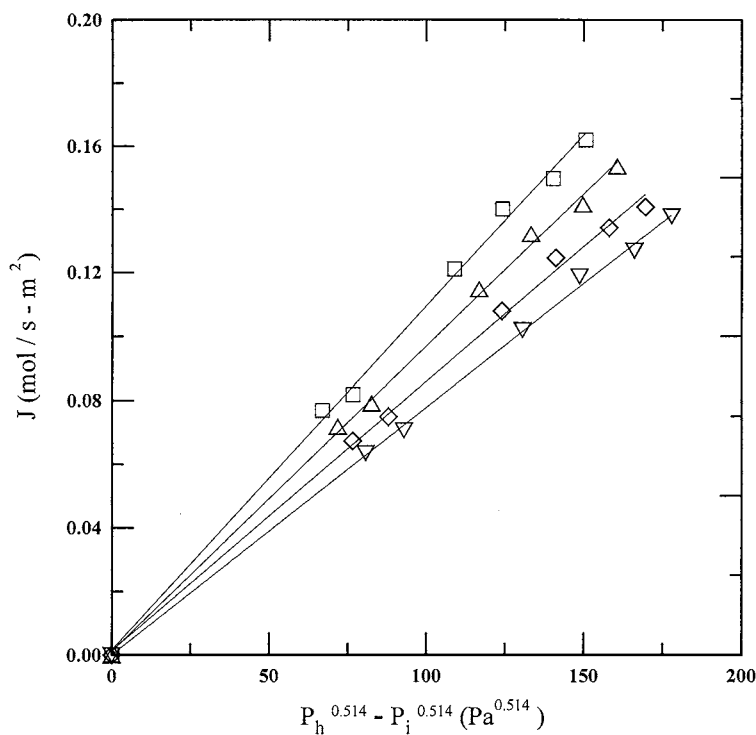


Figure 14. The dependence of hydrogen fluxes on $P_h^n - P_i^n$ at various temperatures through the Pd layer of α -1 membrane. (□) 669 K, (Δ) 647 K, (◇) 625 K, (▽) 600 K.



13, respectively. It can be seen that the pressure exponent was larger than 0.5 value expected by Sievert's law. The n_{grand} values decreased with increasing thickness of Pd layer for the same support, whereas it increased with decreasing the pore size of support for the same thickness of the Pd dense layer. Therefore, the resistance of the support cannot be neglected. In addition, an increase in n indicated that the relative resistance of the support on the overall flow of permeation is increased.

For the bulk Pd layer of Pd/Al₂O₃ composite membranes:

By subtracting the permeation of hydrogen through the α -Al₂O₃ support, the dependence of hydrogen flux through bulk Pd layer of α -1 and α -2 membranes on corrected pressure difference, $P_h^n - P_i^n$, are illustrated in Figures 14 and 15, respectively. The results show that the corrected pressure exponent for α -2 membrane was near 0.5 expected for Sievert's law, indicating the bulk diffusion rate limitation, whereas the thin thickness of Pd layer leads to the exponent higher than 0.5 for α -1 membrane.

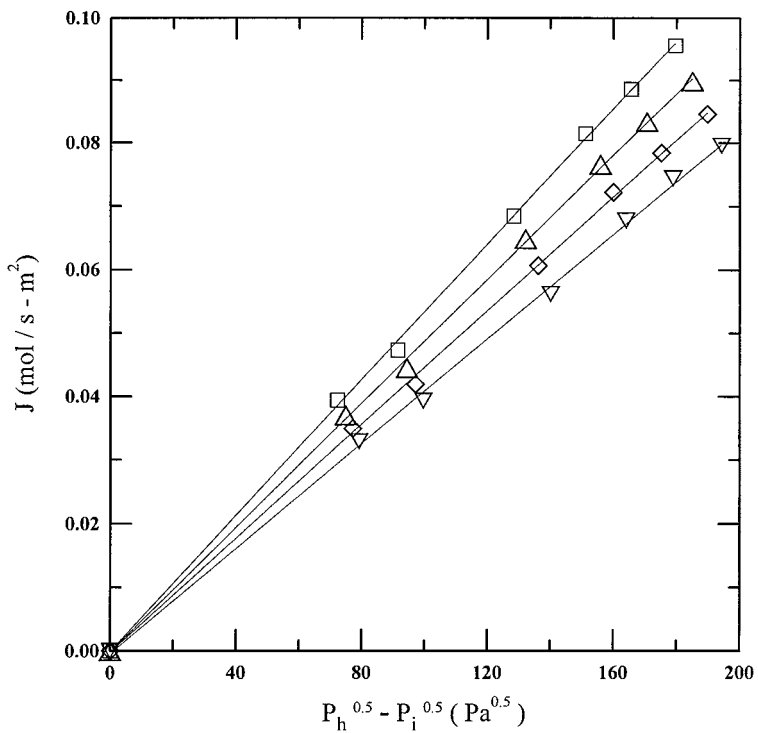


Figure 15. The dependence of hydrogen fluxes on $P_h^n - P_i^n$ at various temperatures through the Pd layer of α -2 membrane. (□) 669 K, (△) 647 K, (◇) 625 K, (▽) 600 K.



Activation Energy of Hydrogen Permeation

For Pd/Al₂O₃ composite membranes:

The effect of temperature on the hydrogen permeability for each membrane showed a linear relationship as illustrated in Figure 16. From the slopes of the straight lines, the activation energies of hydrogen permeation for the α -1, α -2, and γ -2 membranes were evaluated to be 8.73, 8.82, and 9.3 kJ/mol, respectively. These values were approximately in accordance with the data of other studies (2). For the hydrogen permeation through a Pd/Al₂O₃ membrane, the apparent activation energy surely includes the energy barriers for dissolution and diffusion of hydrogen in the Pd layer and the hydrogen permeation in the porous support. Therefore, the activation energies for these membranes with different thickness of palladium layer and different supports might be different. Eventually, the activation energy increases with increasing the mass transfer resistance of support, whereas

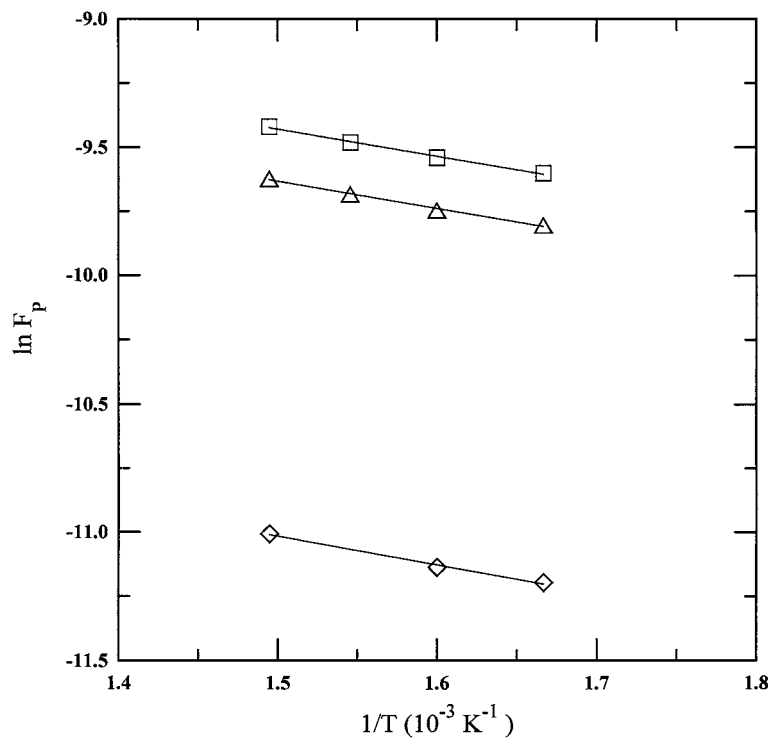


Figure 16. Arrhenius plot of hydrogen permeability through the Pd composite membranes.
 (□) α -1 membrane, (△) α -2 membrane, (◇) γ -2 membrane.



the activation energy doesn't vary with the thickness of Pd dense layer for same support significantly.

For the bulk Pd layer of Pd/Al₂O₃ composite membranes:

Subtracting the transport resistance of the support from overall resistance, the activation energy of hydrogen permeation through the bulk Pd layer of Pd/Al₂O₃ composite membranes was calculated using Equation (12). The activation energy of hydrogen permeation through α -1 and α -2 membranes were determined to be 15.6 and 12.7 kJ/mol, respectively. For α -2 membrane, this value was in good agreement with that of 13.8 kJ/mol for Pd membrane reported by Holleck (18). However, the activation energy of hydrogen permeation through α -1 membrane was larger than through α -2 membrane. We speculate this trend is due to the thin thickness of Pd layer.

CONCLUSIONS

In this study, electroless plating were used to deposit palladium film on the surface of a porous α -Al₂O₃ support and a supported γ -Al₂O₃ membrane, respectively. Permeation behaviors of hydrogen and nitrogen through the α -Al₂O₃ support and the three Pd composite membranes were studied.

For the α -Al₂O₃ support, the permeation of gases can be described by the combined mechanism of Knudsen diffusion and Poiseuille flow. For three Pd composite membranes, the selectivity coefficients of hydrogen to nitrogen approached infinite. The result showed that the deposited Pd layer was defect free. Besides, because the resistance of the support could not be neglected, it showed that the hydrogen fluxes through these Pd composite membranes did not obey Sievert's law. Furthermore, it was better to correlate the hydrogen flux to the difference of permeation pressure using a power higher than 0.5, which was dependent on the support and the thickness of palladium layer.

ACKNOWLEDGMENT

This study was performed under the auspices of the National Science Council of the Republic of China, under contract number NSC85-2214-E006-011, to which the authors wish to express their thanks.

NOMENCLATURE

Ea activation energy of permeability coefficient (kJ mol⁻¹)
 A_0 preexponential (mol m⁻² s⁻¹ Pa⁻ⁿ)



F_p	gas permeability ($\text{mol m}^{-2} \text{ s}^{-1} \text{ Pa}^{-1}$)
F_{Pl}	premultiplication factor ($\text{mol m}^{-2} \text{ s}^{-1} \text{ Pa}^{-n}$)
F_{pk}	gas permeability due to Knudsen diffusion ($\text{mol m}^{-2} \text{ s}^{-1} \text{ Pa}^{-1}$)
$F_{PV} P_{AVE}$	gas permeability due to viscous flow ($\text{mol m}^{-2} \text{ s}^{-1} \text{ Pa}^{-1}$)
J	gas flux ($\text{mol m}^{-2} \text{ s}^{-1}$)
Kn	Knudsen number
L	thickness of membrane (m)
M	molecular weight of gas (g mol^{-1})
P_h, P_l	partial pressure of gas in the sides of high pressure and low pressure of membrane, respectively (Pa)
P_{AVE}	mean pressure (Pa)
P_i	the interface pressure (Pa)
R	gas constant ($8.314 \text{ J mol}^{-1} \text{ K}^{-1}$)
$R_{overall}$	overall resistance ($\text{m}^2 \text{ s Pa mol}^{-1}$)
R_{Pd}	resistance of Pd layer ($\text{m}^2 \text{ s Pa mol}^{-1}$)
R_s	resistance of support ($\text{m}^2 \text{ s Pa mol}^{-1}$)
r	mean pore size (m)
T	temperature (K)

Greek

λ	the pore radius (nm)
α_{ij}^*	the ideal separation factor
μ	viscosity of gas (Pa s)
ε	porosity of a porous medium
τ	tortuosity factor of a porous medium

REFERENCES

- Uemiy, S.; Sato, N.; Ando, H.; Kude, Y.; Matsuda, T.; Kikuchi, E. *J. Membrane Sci.* **1991**, *56*, 303.
- Uemiy, S.; Kugino, Y.; Sato, N.; Matsuda, T.; Kikuchi, E. *J. Membrane Chem. Lett.* **1988**, 1678.
- Shu, J.; Adnot, A.; Grandjean, B.P.A.; Kaliaguine, S. *Thin Solid Film* **1996**, *286*, 72.
- Shu, J.; Grandjean, B.P.A.; Ghali, E.; Kaliaguine, S. *J. Membrane Sci.* **1993**, *77*, 181.
- Mardilovich, P.P.; She, Y.; Ma, Y.H.; Rei, M.H. *AIChE J.* **1998**, *44*, 3102.
- Collins, J.P.; Way, J.D. *Ind. Eng. Chem. Res.* **1993**, *32*, 3006.
- Yeung, K.L.; Varma, A. *AIChE J.* **1995**, *41*, 2131.



8. Li, A.; Xiong, G.; Gu, J.; Zheng, L. *J. Membrane Sci.* **1996**, *110*, 257.
9. Ilias, S.; Su, N.; Udo-Aka, U.I.; King, F.G. *Sep. Sci. Technol.* **1997**, *32*, 487.
10. Shu, J.; Grandjean, B.P.A.; Kaliaguine, S. *Can. J. Chem. Eng.* **1997**, *75*, 712.
11. Zhao, H.B.; Pflanz, K.; Gu, J.H.; Li, A.W.; Stroh, N.; Brunner, H.; Xiong, G.X. *J. Membrane Sci.* **1998**, *142*, 147.
12. Yan, S.; Maeda, H.; Kusakabe, K.; Morooka, S. *Ind. Eng. Chem. Res.* **1994**, *33*, 616.
13. Konno, M.; Shindo, M.; Sugawara, S.; Saito, S. *J. Membrane Sci.* **1988**, *37*, 193.
14. Mason, E.A.; Malinauskas, A.P. *Elsvier*: Amsterdam, 1983.
15. Krishna, R. *Chem. Eng. J.* **1987**, *35*, 75.
16. Huang, T.C.; Chen, H.I. *Sep. Sci. Technol.* **1995**, *30* (10), 2189.
17. Barrer, R.M. *Diffusion in and Through Solid*; Cambridge University Press: London, 1941.
18. Holleck, G.I. *J. Phys. Chem.* **1970**, *74*, 503.
19. Jayaraman, V.; Lin, Y.S. *J. Membrane Sci.* **1991**, *56*, 315.
20. Uemiya, S.; Matsuda, T.; Kikuchi, E. *J. Membrane Sci.* **1991**, *56*, 315.
21. Govind, R.; Atnoor, D. *Ind. Eng. Chem. Res.* **1991**, *30*, 591.
22. Henis, Jay M.S.; Tripodi, M.K. *J. Membrane Sci.* **1981**, *8*, 233.
23. Huang, T.C.; Wei, M.C.; Chen, H.I. *Chem. Eng. Communications* submitted, 2000.
24. Berry, L.G. *Powder Diffraction File*, 4-783 and 5-0681, Joint Committee on Powder Diffraction Standards (JCPDS), Pennsylvania, 1974.
25. Chen, H.I. *Ph.D. Thesis*. National Cheng Kung University, Tainan, Taiwan, 1994.

Received August 5, 1999

Revised June 2000



Request Permission or Order Reprints Instantly!

Interested in copying and sharing this article? In most cases, U.S. Copyright Law requires that you get permission from the article's rightsholder before using copyrighted content.

All information and materials found in this article, including but not limited to text, trademarks, patents, logos, graphics and images (the "Materials"), are the copyrighted works and other forms of intellectual property of Marcel Dekker, Inc., or its licensors. All rights not expressly granted are reserved.

Get permission to lawfully reproduce and distribute the Materials or order reprints quickly and painlessly. Simply click on the "Request Permission/Reprints Here" link below and follow the instructions. Visit the [U.S. Copyright Office](#) for information on Fair Use limitations of U.S. copyright law. Please refer to The Association of American Publishers' (AAP) website for guidelines on [Fair Use in the Classroom](#).

The Materials are for your personal use only and cannot be reformatted, reposted, resold or distributed by electronic means or otherwise without permission from Marcel Dekker, Inc. Marcel Dekker, Inc. grants you the limited right to display the Materials only on your personal computer or personal wireless device, and to copy and download single copies of such Materials provided that any copyright, trademark or other notice appearing on such Materials is also retained by, displayed, copied or downloaded as part of the Materials and is not removed or obscured, and provided you do not edit, modify, alter or enhance the Materials. Please refer to our [Website User Agreement](#) for more details.

Order now!

Reprints of this article can also be ordered at
<http://www.dekker.com/servlet/product/DOI/101081SS100001075>